

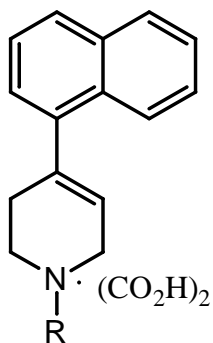
### **Chapter 3. Evaluation of steric parameters that influence substrate and inhibitor properties of C-4 substituted tetrahydropyridines**

Little is known regarding the structural features of the MAO-A and B active sites which lead to the selectivities observed with various substrates and inhibitors. Understanding the factors responsible for these selectivities could prove useful in the design of drugs to target the enzymes. MPTP and its analogs provide an opportunity to probe the active sites of these biologically important enzymes. Studies on the interactions of tetrahydropyridines with MAO also are prompted by the MAO catalyzed bioactivation of MPTP and some of its analogs to generate neurotoxic metabolites.<sup>236,237</sup>

In order to evaluate the steric limits present in the active sites of MAO-A and B and to carry out a topological analysis of the active sites using SAR, we have employed a series of semirigid MPTP analogs. Analogs of MPTP with direct substitution on the phenyl ring that have been examined in vitro with MAO-A and B are summarized in Table 2, section 2.2. Small groups such as a halogen, methyl, ethyl, or nitro group have been introduced about the phenyl ring of MPTP in the *ortho*, *meta*, or *para* -position. We have designed a series of substituted MPTP analogs to evaluate the steric effects produced by bulkier, less flexible substituents at the C4 position. In an attempt to examine inhibitor selectivity and evaluate possible relationships between the factors that effect substrate and inhibitor enzyme selectivity, a series of mechanism based inactivators also were prepared. Specifically, in the effort to characterize the spacial features that may contribute to enzyme selectivity, we have determined

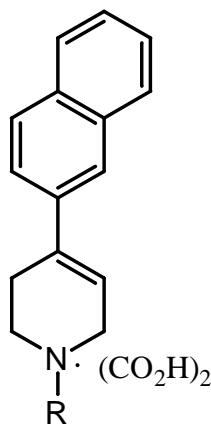
the  $K_m$  and  $V_{max}$  values for the MAO-A and MAO-B catalyzed oxidations of 1-methyl-1,2,3,6-tetrahydropyridinyl derivatives bearing various aryl groups at C4 (Chart 4). The C-4 substituted analogs include the 3-indolyl (**147**), the *ortho*-, *meta*-, and *para*-phenyl substituted MPTP analogs (**131-133**). For comparison, we have included the previously reported  $\alpha$ -naphthyl (**134**) and  $\beta$ -naphthyl (**135**) analogs.<sup>148</sup> In a parallel series we have examined the  $k_{inact}$  and  $K_i$  values for the corresponding 1-cyclopropyl analogs which, based on the results of earlier studies, were expected to be mechanism based inactivators of these enzymes. The data generated from these studies have been used to analyze the relative topology of the MAO-A and B active sites using computer assisted molecular modeling. The semi-empirical AM1 method<sup>247</sup> was used to generate the minimum energy conformers and the display software Mac Mimic (Instar Software, version 91) was utilized to generate the van der Waals volumes of the compounds. Overlay and comparison of these volumes generated images of the topological features of the two active sites.

**Chart 4.** A Series of 1-Methyl and 1-Cyclopropyl-4-Aryl-Substituted Tetrahydropyridines.



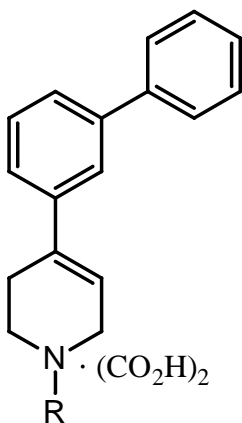
R = CH<sub>3</sub>, (134)

R =  $\triangle$ , (139)



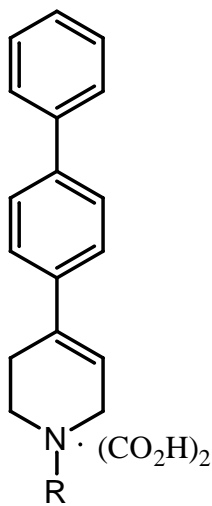
R = CH<sub>3</sub>, (135)

R =  $\triangle$ , (140)



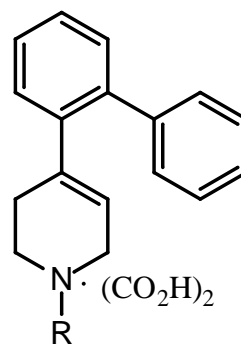
R = CH<sub>3</sub>, (132)

R =  $\triangle$ , (137)



R = CH<sub>3</sub>, (131)

R =  $\triangle$ , (136)



R = CH<sub>3</sub>, (133)

R =  $\triangle$ , (138)

### 3.1. 1-Methyl and 1-cyclopropyl-4-biphenyl substituted tetrahydropyridines

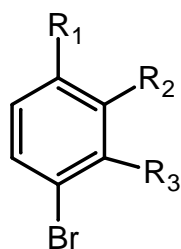
### 3.2 Chemistry

The synthesis of 1-methyl-4-(4'-phenylphenyl)-1,2,3,6-tetrahydropyridine (**131**) proceeded via the Grignard formation of the commercially available 4-bromobiphenyl (**114**) followed by condensation of the Grignard with the 1-methyl-4-piperidone (**119**) to yield the 1-methyl-4-(4'-phenylphenyl)-4-piperidinol (**121**, Scheme 8a). The tetrahydropyridine **131** was obtained by acid catalyzed dehydration of **121** in a 1:3 mixture of hydrochloric acid and acetic acid at reflux and characterized as its stable oxalate salt. (Scheme 8b). The 1-methyl-4-(3'-phenylphenyl)-1,2,3,6-tetrahydropyridine (**132**) was prepared in the same manner using the available starting material 3-bromobiphenyl (**115**). We attempted to synthesize the 1-methyl-4-(2'-phenylphenyl)-1,2,3,6-tetrahydropyridine (**133**) in the same manner using the starting compound 2-bromobiphenyl (**116**), but obtained very poor yields (8-15%) which appear to be due to the steric interference of the *ortho* phenyl substituent on Grignard formation. The synthesis was modified to obtain **133** by first generating the organolithium reagent of **116** using *n*-butyllithium followed by condensation with **119** which gave 1-methyl-4-(2-phenylphenyl)-4-piperidinol (**123**) in 78% yield. The subsequent dehydration and salt formation with oxalic acid gave the desired MPTP derivative **133**. The naphthyl analogs **134** and **135** were prepared using the previously reported method.<sup>148</sup>

Synthesis of the 1-cyclopropyl mechanism based inactivators (**136-140**) began with the synthesis of 1-cyclopropyl-4-piperidone as previously described

(**120**, Scheme 9).<sup>238</sup> Using the same methodology as described previously for the N-methyl derivatives, the condensation reaction of **120** with the organometallic derivative of the commercially available starting materials **114-118**, followed by dehydration and salt formation yielded the desired N-cyclopropyl analogs **136-140**.

**Scheme 8a.** Synthesis of C4 Substituted Piperidinols (**121 - 130**)



**114 - 118**

$R_1 = \text{Ph} ; R_2, R_3 = \text{H}$  (**114**)

$R_2 = \text{Ph} ; R_1, R_3 = \text{H}$  (**115**)

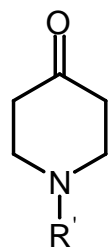
$R_3 = \text{Ph} ; R_1, R_2 = \text{H}$  (**116**)

$R_2, R_3 = (-\text{CH}=\text{CH}-\text{CH}=\text{CH}-) ; R_1 = \text{H}$  (**117**)

$R_1, R_2 = (-\text{CH}=\text{CH}-\text{CH}=\text{CH}-) ; R_3 = \text{H}$  (**118**)

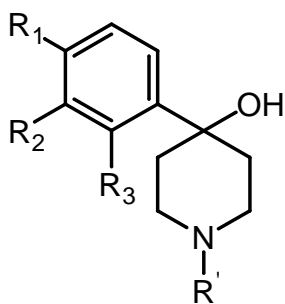
1. n-BuLi / THF  
or Mg / THF

2.



$R' = \text{CH}_3$  (**119**)

$R' = \text{cyclopropyl}$  (**120**)



**121-130**

$R' = \text{CH}_3, R_1 = \text{Ph}, R_2 = R_3 = \text{H}$  (**121**)

$R' = \text{CH}_3, R_2 = \text{Ph}, R_1 = R_3 = \text{H}$  (**122**)

$R' = \text{CH}_3, R_3 = \text{Ph}, R_1 = R_2 = \text{H}$  (**123**)

$R' = \text{CH}_3, R_2, R_3 = (-\text{CH}=\text{CH}-\text{CH}=\text{CH}-) ; R_1 = \text{H}$  (**124**)

$R' = \text{CH}_3, R_1, R_2 = (-\text{CH}=\text{CH}-\text{CH}=\text{CH}-) ; R_3 = \text{H}$  (**125**)

$R' = \text{cyclopropyl}, R_1 = \text{Ph}, R_2 = R_3 = \text{H}$  (**126**)

$R' = \text{cyclopropyl}, R_2 = \text{Ph}, R_1 = R_3 = \text{H}$  (**127**)

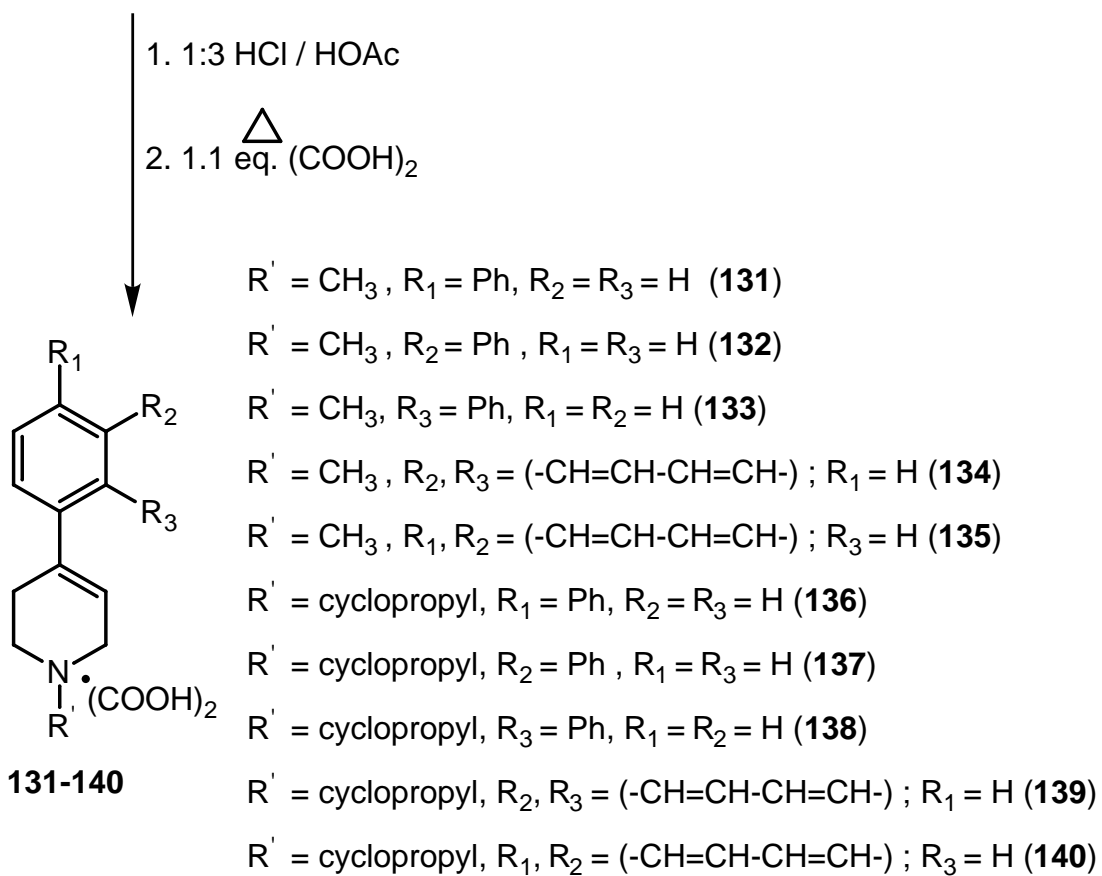
$R' = \text{cyclopropyl}, R_3 = \text{Ph}, R_1 = R_2 = \text{H}$  (**128**)

$R' = \text{cyclopropyl}, R_2, R_3 = (-\text{CH}=\text{CH}-\text{CH}=\text{CH}-) ; R_1 = \text{H}$  (**129**)

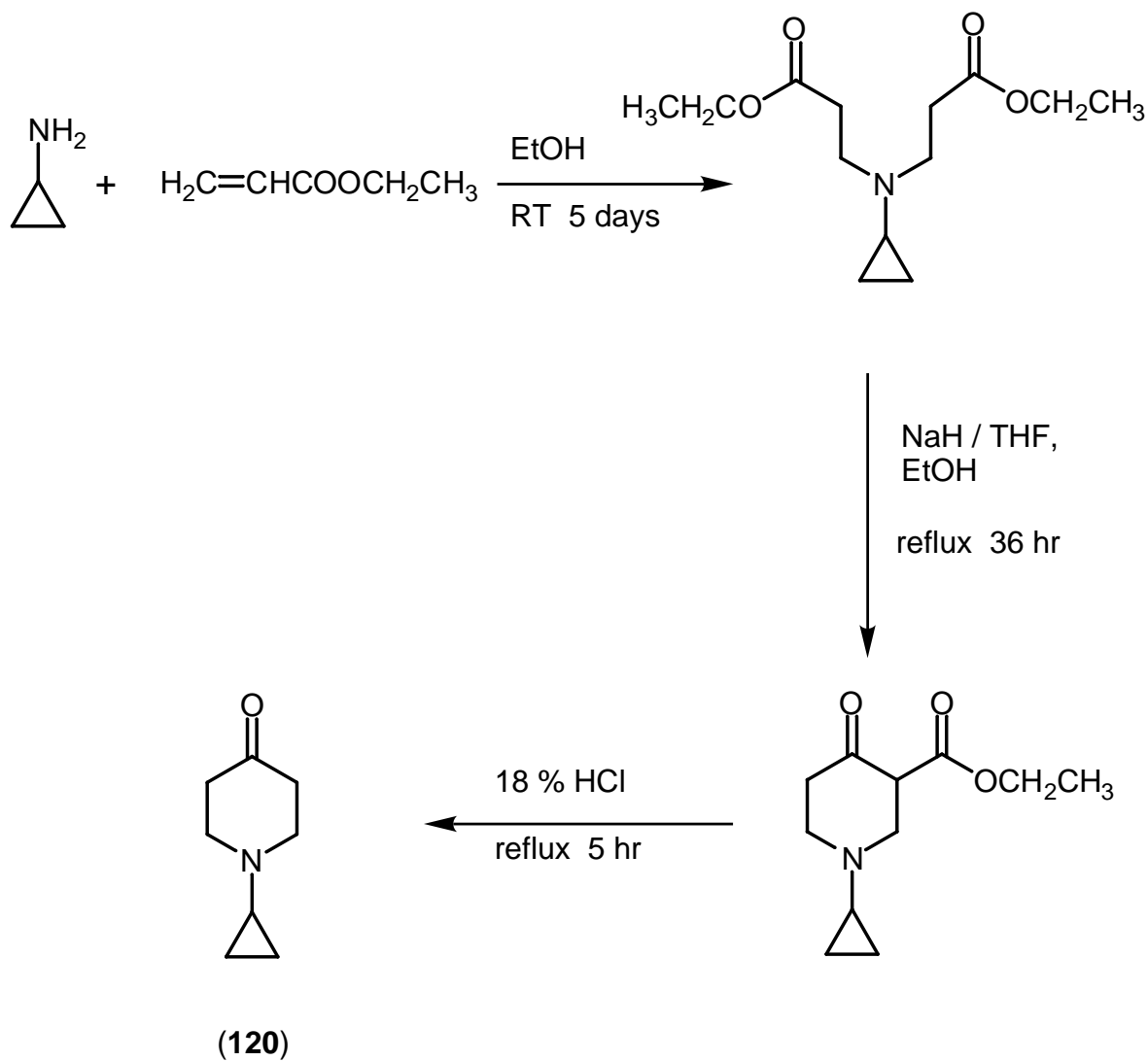
$R' = \text{cyclopropyl}, R_1, R_2 = (-\text{CH}=\text{CH}-\text{CH}=\text{CH}-) ; R_3 = \text{H}$  (**130**)

**Scheme 8b.** Synthesis of C4 Substituted Tetrahydropyridine Analogs (**132 - 140**)

**121-130** (Scheme 8a)



**Scheme 9.** Synthesis of 1-Cyclopropyl-4-piperidone



**3.3. Enzymology**

The lack of water solubility of compounds **131-140** made it difficult to do enzymology on these MPTP analogs. Woo and Silverman<sup>239</sup> have reported that organic solvents such as benzene or dimethyl sulfoxide (DMSO) do not

dramatically affect the catalytic activities of MAO. Therefore, we decided to use 100 mM phosphate buffer (pH = 7.4) containing DMSO to help solubilize the compounds. A systematic evaluation of the effects of DMSO on enzyme kinetics was performed with both MAO-A and MAO-B. An experiment was done to determine the percentage of enzyme activity remaining as a function of the amount of DMSO present. Solutions of MPTP (5 M) were prepared in 100 mM phosphate buffer containing 0 - 20% DMSO. These solutions were incubated with MAO-B and the rate of oxidation determined. The same experiment was done for MAO-A using the known substrate 1-methyl-4-phenoxy-1,2,3,6-tetrahydropyridine (**88**, 1 M). The results are summarized in Table 3.

**Table 3.** Summary of the Effect of DMSO on the Ability of MAO to Catalyze the Oxidation of a Substrate.

% DMSO	% Remaining MAO-B Activity	% Remaining MAO-A Activity
0	100	100
5	90	92
10	90	85
15	83	75
20	60	72

Based on these results, we decided to use 10% DMSO to do the following kinetic and inhibition studies with the MPTP derivatives **131-140**.

UV scans of a 1.0 mM solution of 1-methyl-4-(4-phenylphenyl)-1,2,3,6-tetrahydropyridine (**131**) in the presence of 0.08  $\mu$ M MAO-B at 30 °C revealed that there was no detectable MAO-B substrate activity with this compound. The

scans of **131** with 0.16  $\mu\text{M}$  MAO-A also revealed that this analog had no MAO-A substrate properties.

UV scans of a 0.5 mM solution of 1-methyl-4-(3-phenylphenyl)-1,2,3,6-tetrahydropyridine (**132**) in the presence of 0.08  $\mu\text{M}$  MAO-B at 30 °C revealed the time-dependent formation of a chromophore with maximal absorption at 340 nm (Figure 3). The chromophore at 340 nm rapidly shifted to a wavelength of 305 nm which we believe to be the pyridinium species **142**. The kinetic analysis of the substrate properties of **132** with 0.08  $\mu\text{M}$  MAO-B (activity 9.0 nmol/mL) was performed by monitoring the dihydropyridinium product **141** at 340 nm at initial substrate concentrations of 1.0 mM, 0.5 mM, 0.25 mM, and 0.125 mM. The Lineweaver-Burke analysis of the data using the following equation:

$$v \left( \frac{\text{nmoles}}{\text{ml} \cdot \text{min}} \right) = \frac{\left[ \frac{\Delta\text{OD}}{\epsilon} \times 10^6 \right] \times \text{total Volume of incubate}}{\text{enzyme volume}}$$

yielded the double reciprocal plot in Figure 4, from which we obtained the  $V_{\text{max}}$  and  $K_{\text{m}}$  values. The velocity ( $v$ ) was calculated for each substrate concentration examined with respect to enzyme concentrations used in the experiments. The rate of product formation as measured by  $\Delta\text{OD}$  is divided by the estimated  $\epsilon$  value (16000) for the dihydropyridinium product formed. Taking  $V_{\text{max}}/K_{\text{m}}$  as an overall estimate of the efficiency of catalysis, the substrate activity of **132** was  $157 \text{ min}^{-1}\text{mM}^{-1}$  (Table 5). The UV scans of **132** with MAO-B (Figure 3) indicated that the growth of the chromophore at 340 nm was not exponential which led us to suspect that the product of enzyme catalysis may be inactivating the enzyme. But even at inhibitor concentrations of 1 mM, no

MAO-B inactivation properties could be detected. Metabolites of compound **132** could be inhibiting enzyme catalysis via competitive inhibition, which should be looked at more closely. The scans of **132** with 0.16  $\mu\text{M}$  MAO-A at a substrate concentration of 1.0 mM revealed that this analog had no detectable MAO-A substrate properties. Therefore, analog **132** is exclusively an MAO-B substrate.

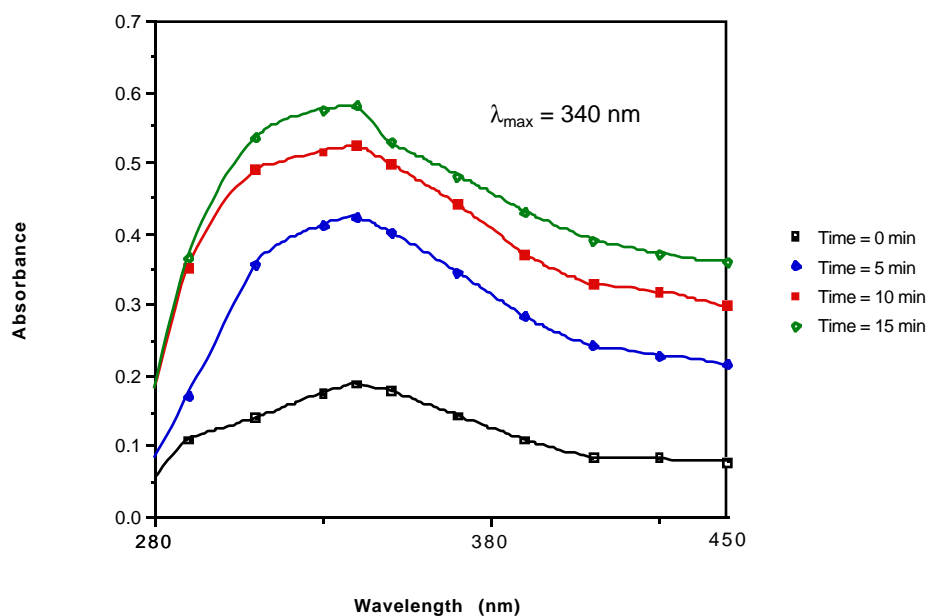


**Figure 3.** UV Scans of an Incubation Mixture Containing 0.5 mM 1-methyl-4-(3'-phenylphenyl)-1,2,3,6-tetrahydropyridine and 0.08  $\mu\text{M}$  MAO-B

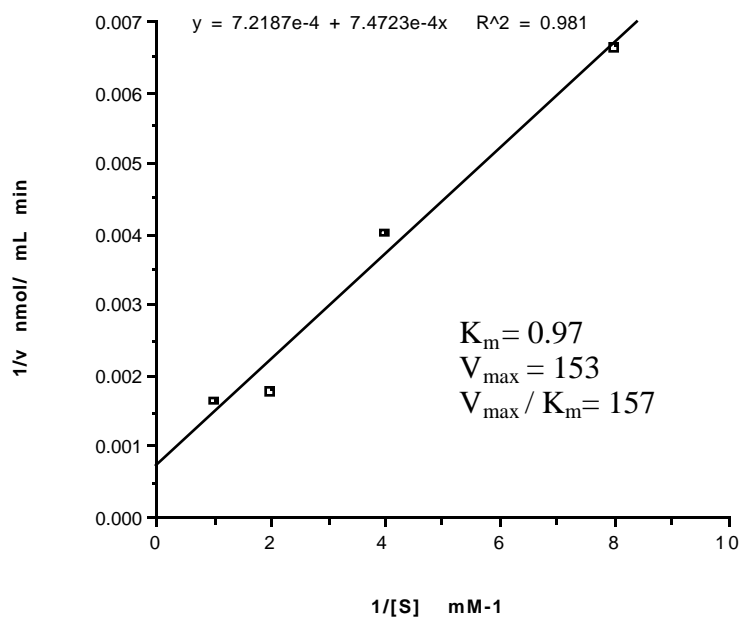
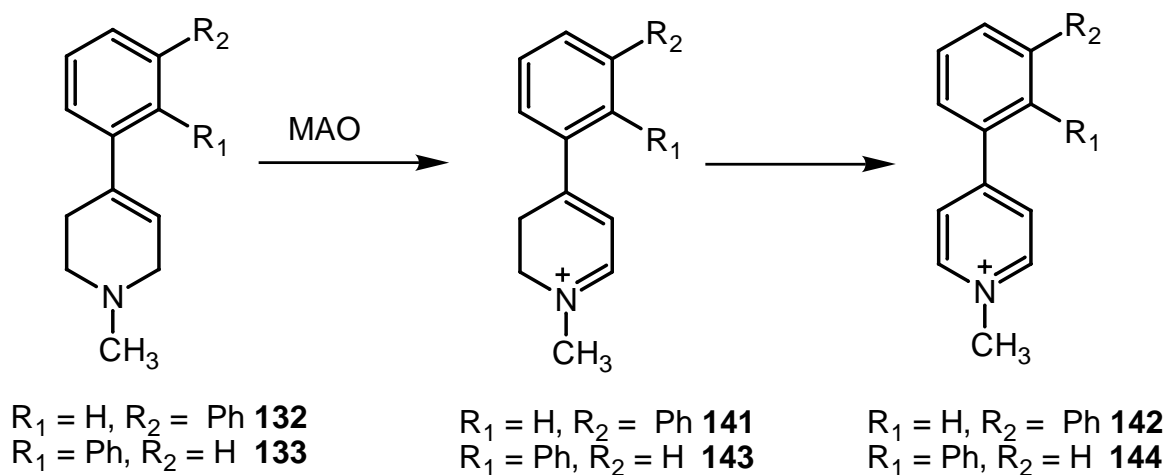


**Figure 4.** The Lineweaver-Burke Double Reciprocal Plot for the MAO-B Catalyzed Oxidation of 1-Methyl-4-(3-phenylphenyl)-1,2,3,6-tetrahydropyridine (**132**)

**Scheme 10.** Metabolic Fate of **132** and **133** when incubated with MAO.



Incubation of a 1.0 mM solution of 1-methyl-4-(2-phenylphenyl)-1,2,3,6-tetrahydropyridine (**133**) in the presence of 0.08  $\mu\text{M}$  MAO-B at 30 °C and scanning the incubation mixture by UV spectrometry every 5 minutes for a 30 minute period revealed the time-dependent formation of a chromophore with maximal absorption at 325 nm. The kinetic analysis of substrate activity of **133** with 0.08  $\mu\text{M}$  MAO-B (activity 9.0 nmol/mL), performed by monitoring the dihydropyridinium product formation (**143**) at  $\lambda_{\text{max}} = 325$  nm at substrate concentrations of 2.0 mM, 1.5 mM, 1.0 mM, and 0.5 mM, revealed the fact that the substrate activity was very poor. From the Lineweaver-Burke analysis of the data, we obtained a  $V_{\text{max}} = 20 \text{ min}^{-1}$ , a very high  $K_{\text{m}}$  of 1.7 mM, and the resulting  $V_{\text{max}}/K_{\text{m}} = 12 (\text{min}\cdot\text{mM})^{-1}$  (Table 5).

UV scans of a 1.0 mM solution of **133** in the presence of 0.16  $\mu\text{M}$  MAO-A (activity 7.0 nmol/mL) at 30 °C revealed the time-dependent formation of the same chromophore at 325 nm, as observed with MAO-B, which rapidly shifted to a chromophore suspected to be the pyridinium species **144** which absorbs at 294 nm. The MAO-A substrate activity, however, appeared to be very good. The kinetic analysis of substrate activity of **133** with 0.16  $\mu\text{M}$  MAO-A at concentrations of 1.0 mM, and 0.5 mM, .025 mM, and 0.125 mM, (Experiment A-D, respectively, Table 4), monitoring spectrophotometrically the formation of the chromophore at 325, yielded the results summarized in Table 4. As the dihydropyridinium species **143** was not available synthetically, the  $\epsilon$  value used to calculate the kinetic parameters was that of MPTP, which is 16,000. The Lineweaver-Burke analysis of the data yielded the double reciprocal plot shown in Figure 5 from which we obtained the kinetic parameters. For analog **133** the  $V_{\text{max}}$  is  $107 \text{ min}^{-1}$ ,  $K_{\text{m}}$  is 0.12 mM, resulting in a  $V_{\text{max}}/K_{\text{m}} = 892$

(min·mM)<sup>-1</sup> (Table 5).

**Table 4.** Kinetic Data Obtained for the MAO-A Catalyzed Oxidation of 1-Methyl-4-(2-phenylphenyl)-1,2,3,6-tetrahydropyridine (**133**)

Experiment	1/ [substrate] mM <sup>-1</sup>	Avg. rate (n=3) absorbance/min	Rate nmol/mL · min
A	1	0.1573	657.1
B	2	0.1453	605.4
C	4	0.1217	507.2
D	8	0.0919	383.0

The UV scans of the incubation of the  $\alpha$ -naphthyl analog **134** and the  $\beta$ -naphthyl analog **135** with 0.08  $\mu$ M MAO-B or 0.16  $\mu$ M MAO-A revealed the time-dependent formation of chromophores at 316 nm and 328 nm, respectively. The kinetic analysis of **134** and **135** with MAO-B established that both analogs were MAO-B substrates yielding  $V_{\max}/K_m$  values of 364 and 71  $\text{min}^{-1}\text{mM}^{-1}$ , respectively (Table 5). The substrate studies of **134** and **135** with MAO-A revealed that these naphthyl analogs were better substrates for MAO-A than -B. From the Lineweaver-Burke analysis we obtained a  $V_{\max}/K_m$  of 862  $\text{min}^{-1}\text{mM}^{-1}$  for the  $\alpha$ -naphthyl analog **134** and a  $V_{\max}/K_m$  of 443  $\text{min}^{-1}\text{mM}^{-1}$  for the  $\beta$ -naphthyl analog **135** (Table 5). Comparison of the results obtained for the two naphthyl derivatives **134** and **135** with those reported in the literature<sup>148</sup> (Table 5) point out the importance of the enzyme source. Particularly impressive are the differences observed here between extracted

human placental MAO-A and recombinant MAO-A from human liver expressed in yeast.<sup>148</sup> These differences are unlikely to originate from the methods used because the results obtained with MAO-B, extracted from beef liver in both cases, are comparable.

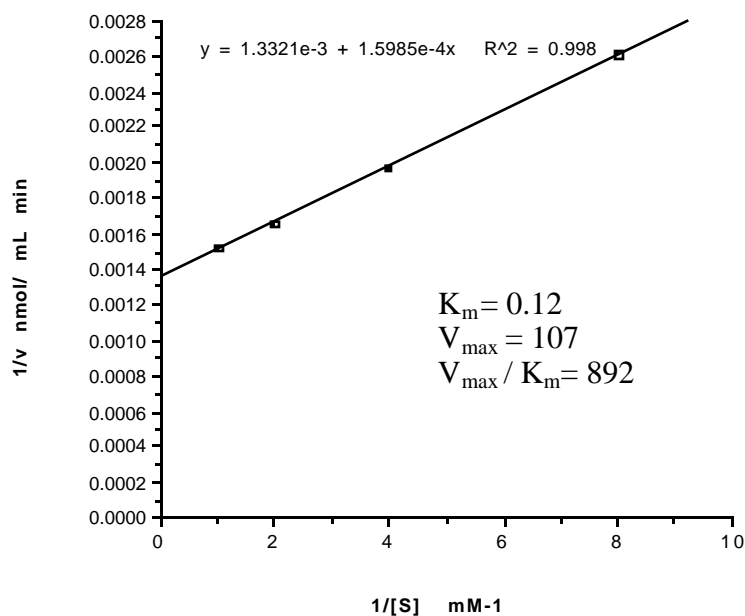


**Figure 5.** The Lineweaver-Burke Double Reciprocal Plot for the MAO-A Catalyzed Oxidation of 1-Methyl-4-(2-phenylphenyl)-1,2,3,6-tetrahydropyridine

**Table 5.**  $V_{\max}$  and  $K_m$  Values for the MAO-A and MAO-B Catalyzed Oxidation of Various 4-Aryl-1-methyl-1,2,3,6-tetrahydropyridine Derivatives

Cmpd.	MAO-A			MAO-B			$SC_{A/B}^b$
	$V_{\max}$	$K_m$	$V_{\max}/K_m$	$V_{\max}$	$K_m$	$V_{\max}/K_m$	
<b>3</b>	20	0.14	143	204	0.39	523	0.27
<b>131</b>		NSD <sup>a</sup>			NSD		--
<b>132</b>		NSD		153	0.97	157	--
<b>133</b>	107	0.12	892	20	1.7	12	74.33
<b>134</b>	526	0.61	862(1893)	51	0.14	364 (500)	2.37
<b>135</b>	204	0.46	443(2216)	42	0.59	71 (101)	6.24

<sup>a</sup> NSD = No substrate properties detected. In parentheses are values reported in the literature.<sup>148</sup> <sup>b</sup> SC = Selectivity coefficient.

The inactivation studies with **136** - **140** showed that all of the N-cyclopropyl analogs were weak time and concentration dependent inhibitors of MAO-A and -B relative to 1-cyclopropyl-4-phenyl-1,2,3,6-tetrahydropyridine (**145**, CPTP, Table 6). The proposed mechanism for the inactivation of CPTP by the currently accepted SET mechanism is illustrated in Scheme 11. It is probable that the N-cyclopropyl analogs **136** - **140** inactivate the enzyme by a similar enzyme mediated pathway. The MAO-B inactivation studies are carried out by incubating a known concentration of inhibitor with a known enzyme concentration at 30 °C. An aliquot (10  $\mu$ L) from the incubation mixture is added to MPTP (5 mM, 490  $\mu$ L). We monitor spectrophotometrically the increment in the dihydropyridinium metabolite MPDP<sup>+</sup> at  $\lambda$  = 343 nm every 3 sec for 2 min.

The same type of experiment is carried out for MAO-A using as the substrate a 1mM solution of 1-methyl-4-phenoxy-1,2,3,6-tetrahydropyridine (**88**). We determine the rate of oxidation of **88** by monitoring the formation of aminoenone at  $\lambda = 324 \text{ nm}$ .<sup>240</sup> In each case a control experiment was done in which the enzyme is incubated with 100 mM phosphate buffer (pH = 7.4). An aliquot is removed and incubated with the MAO-A or MAO-B substrate in the same manner as described above.

Of the cyclopropyl series, the 1-cyclopropyl-4-( $\alpha$ -naphthyl)-1,2,3,6-tetrahydropyridine (**139**) was one of the better inactivators for MAO-A and illustrates the typical result obtained in an inactivation study. Using various inhibitor concentrations of **139** at 30 °C (1.0 mM, 0.5 mM, 0.25 mM and 0.125 mM) one can estimate the percent remaining enzyme activity relative to control. A plot of the natural log (ln) of the percent remaining activity versus time yielded the graph shown in Figure 6. Estimates of the  $k_{\text{inact}}/K_I$  value for the  $\alpha$ -naphthyl analog (**139**) were obtained by doing a double reciprocal analysis of the data to obtain the plot shown in Figure 7. The  $k_{\text{inact}}/K_I$  values for the remaining N-cyclopropyl analogs were estimated in a similar manner and are reported in Table 6.

Solutions (2 mM) of the cyclopropyl analogs **136** - **140** were incubated in the presence of 0.08  $\mu\text{M}$  MAO-B or 0.16  $\mu\text{M}$  of MAO-A and scanned spectrophotometrically to determine the possibility of substrate activity. None of the analogs showed evidence of dihydropyridinium or pyridinium formation under these conditions.

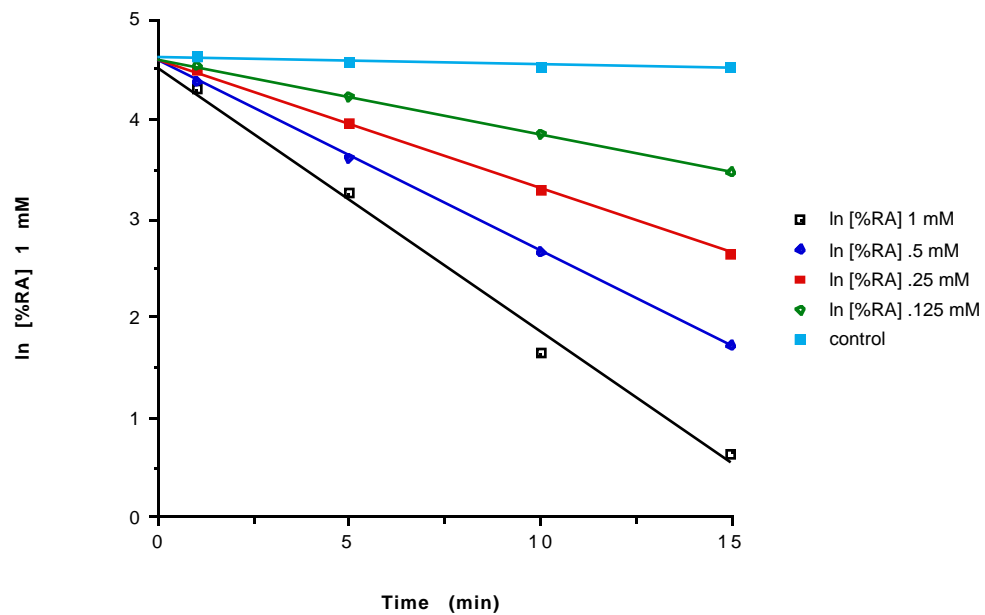


**Figure 6.** Plot of ln [% enzyme activity remaining] Versus Time for the MAO-A Inactivation by 1-Cyclopropyl-4-( $\alpha$ -naphthyl)-1,2,3,6-tetrahydropyridine

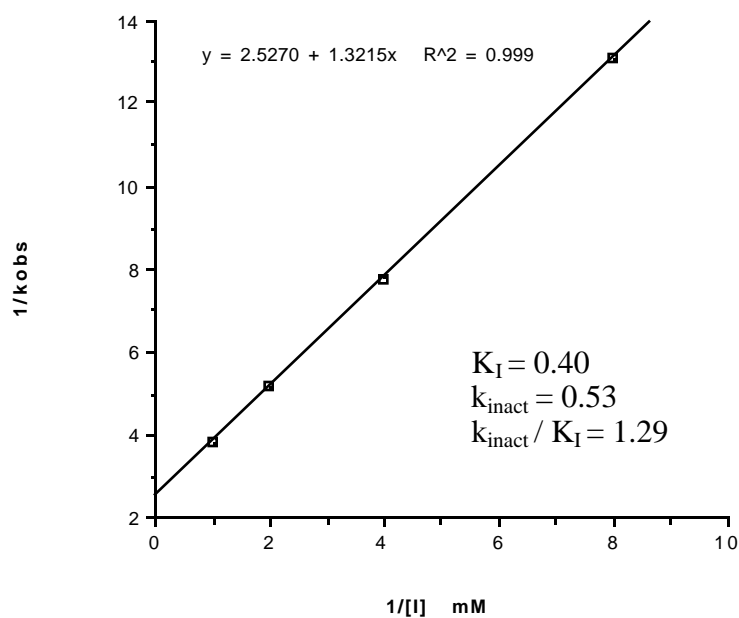


**Figure 7.** The Double Reciprocal Plot for the MAO-A Inactivation by 1-Methyl-4-( $\alpha$ -naphthyl)-1,2,3,6-tetrahydropyridine

**Scheme 11.** Proposed SET Pathway for the Inactivation of MAO by 1-Cyclopropyl-4-phenyl-1,2,3,6-tetrahydropyridine (**145**)

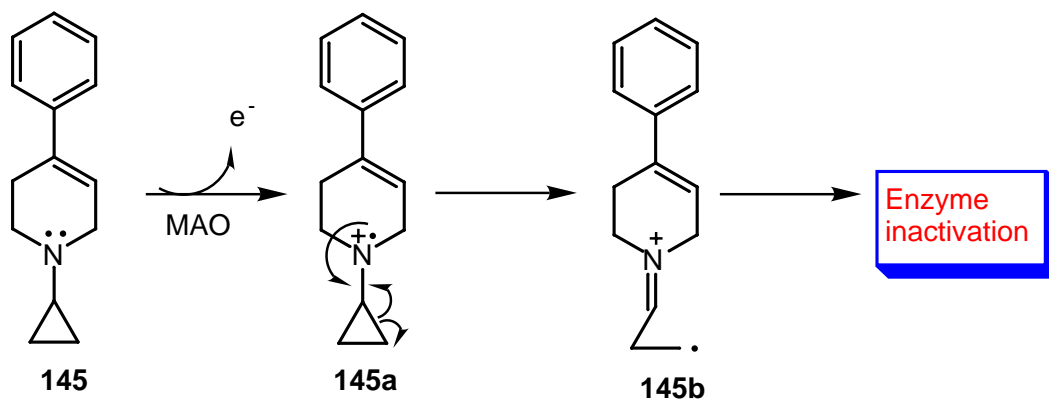


**Table 6.**  $K_i$  and  $k_{inact}$  Values for the Inactivation of MAO-A and MAO-B by Various 4-Aryl-1-cyclopropyl-1,2,3,6-tetrahydropyridine Derivatives.

Cmpd.	MAO-A			MAO-B			$SC_{A/B}^b$
	$k_{inact}$	$K_i$	$k_{inact}/K_i$	$k_{inact}$	$K_i$	$k_{inact}/K_i$	
<b>136</b>		NID <sup>a</sup>			NID		--
<b>137</b>	0.02	0.68	0.03	0.02	0.44	0.05	
<b>138</b>	0.13	0.22	0.59		NID		--
<b>139</b>	0.53	0.40	1.29	0.09	0.11	0.61	1.59
<b>140</b>	0.29	0.38	0.76	0.12	0.15	0.61	1.25
<b>145</b>	0.20	0.05	4.00	0.70	0.18	3.85 <sup>b</sup>	--

<sup>a</sup> NID = No inactivation properties detected. <sup>b</sup> At 37 °C.<sup>241</sup> <sup>b</sup> SC = Selectivity coefficient.

### 3.4 Discussion

The kinetic results obtained with this series of 1-methyl-4-substituted tetrahydropyridinyl analogs (**131** - **135**) are consistent with the previous trends observed and reported in the literature. Since these analogs are rigid and bulky, they provide valuable information about the size limits of the MAO-A and MAO-B active sites. Table 5, where the selectivity coefficient ( $SC_{A/B}$ ) represents the  $V_{max}/K_m$  ratios for MAO-A/MAO-B, summarizes the kinetic results obtained for analogs **131** - **135**. The *p*-biphenyl analog **131** is devoid of both MAO-A and MAO-B substrate properties. This behavior is consistent with the general restriction observed for MAO-B with molecules measuring greater than

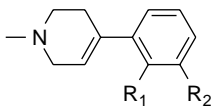
12 Å along the N<sub>1</sub> – C<sub>4</sub> axis.<sup>197</sup> The *m*-biphenyl analog **132** shows weak substrate properties for MAO-B only. This selectivity for MAO-B is expected on the basis of previous literature data<sup>242,243</sup> with various *meta*-substituted MPTP analogs (Table 7) that showed a loss of MAO-A substrate activity with substituents as small as a methoxy group (**43**). The 4-(2-phenyl)phenyl-, 4- $\alpha$ -naphthyl-, and 4- $\beta$ -naphthyl-1-methyl-1,2,3,6-tetrahydropyridinyl analogs (**133**, **134** and **135**, respectively) proved to be substrates for both MAO-A and MAO-B. In all three cases preference was found for the A form, i.e.  $SC_{A/B} > 1$  for these compounds. The greatest MAO-A selectivity is observed with the very bulky *o*-biphenyl analog **123** with  $SC_{A/B}$  of 74. This selectivity reflects the very poor MAO-B substrate properties of this compound and is consistent with the trend of enzyme activity and selectivity observed previously with various *ortho*-substituted MPTP derivatives (Table 7). This was interpreted as a consequence of steric restrictions within the active site of MAO-B that are not present in the active site of MAO-A.<sup>151,191,196</sup>

None of the N-cyclopropyl analogs, **136** - **140**, displayed substrate properties for either form of the enzyme. This is in agreement with the general observation that replacement of the N-methyl group of MPTP with a larger substituent leads to loss of good substrate properties.<sup>197,244,245</sup> Additionally, some cyclopropylamines are mechanism based inactivators of MAO-A and MAO-B<sup>169,241</sup> and often the enzyme is inactivated too rapidly to allow detectable product formation.<sup>153</sup> On the other hand, it has been found that several 4-aryl and 4-aryloxy-1-cyclopropyltetrahydropyridinyl derivatives are good to excellent MAO-B substrates.<sup>189</sup> The factors which control the partition ratio (number of substrate molecules converted to product per inactivation

event) for these compounds remain to be determined.

Several of the 1-cyclopropyltetrahydropyridines prepared in this study were time and concentration dependent inactivators of MAO-A and MAO-B with  $k_{\text{inact}}/K_i$  values ranging from 0.03 to 1.29  $\text{min}^{-1}\text{mM}^{-1}$  (Table 6). The selectivities observed with the inhibitor series of the biphenyl analogs **136** - **138** parallel the selectivities of the corresponding substrates. For example, the *p*-biphenyl analog **136** apparently does not have access to the active site of either enzyme since it displayed no inactivator properties, behavior that parallels that observed with the N-methyl analog **131** which was not a substrate for either enzyme. The *m*-biphenyl analog **137** inhibited MAO-B preferentially while the N-methyl analog **132** was a selective MAO-B substrate. The high  $SC_{A/B}$  value for the *o*-biphenyl N-methyl substrate **133** also is reflected in the MAO-A selective inhibition properties of **138**. The 4- $\alpha$ -naphthyl (**139**) and 4- $\beta$ -naphthyl (**140**) analogs proved to be effective inactivators of both MAO-A and MAO-B while the N-methyl analogs **134** and **135** were substrates for both enzymes although the  $SC_{A/B}$  values are higher for the substrates than for the inhibitors. Thus, although the selectivity for MAO-A or MAO-B is conserved in the N-methyl series and the N-cyclopropyl series, there is no quantitative correlation between substrate and inactivator properties for these series of compounds. In other words, a good substrate will not necessarily lead to an efficient inactivator when the N-methyl is replaced by an N-cyclopropyl group.

**Table 7.** MAO-A and MAO-B Kinetic Data ( $V_{\max}/K_m$ ,  $\text{min}^{-1}\text{mM}^{-1}$ ) of Various *meta*- and *ortho*-Phenyl Substituted MPTP Analogs.<sup>191</sup>

			MAO-A	MAO-B	$SC_{A/B}^b$	$SC_{B/A}^b$
	R <sub>1</sub>	R <sub>2</sub>				
<b>3</b>	H	H	144	525	0.27	3.65
<b>31</b>	2-Me	H	588	1288	0.46	2.19
<b>32</b>	2-Et	H	692	295	2.35	.43
<b>38</b>	2- <i>i</i> Pr	H	1122	51	22.0	0.05
<b>39</b>	H	3-Me	76	646	0.12	8.50
<b>43</b>	H	3-OMe	NSD <sup>a</sup>	933	--	--

<sup>a</sup> NSD = No substrate properties detected. <sup>b</sup> SC = Selectivity coefficient.

### 3.5 Molecular modeling of the biphenyl series

#### 3.5.1. Topological analysis of the MAO-A and MAO-B active sites

We have used the results of these enzyme studies to perform a topological analysis in an attempt to describe some of the structural features of the active sites of MAO-A and MAO-B. We are not attempting to generate complete models in this preliminary analysis and therefore compounds from other series were not included in this study. The minimum energy conformers were generated using the semi-empirical method AM1.<sup>246-248</sup> The van der Waals volumes about the superimposed minimum energy conformers of these

tetrahydropyridinyl analogs (**131** - **135**) were generated using the molecular mechanics program Mac Mimic. The analogs were superimposed using the N1-C6-C5 atoms based on the assumption that the catalytic site of oxidation for the amines must be in the same region in the active site. The van der Waals volumes about these superimposed analogs were used to define the regions about the MPTP skeleton that are allowed and disallowed for substrate/inhibitor and non-substrate/non-inhibitor properties for MAO-A (Figure 8) and MAO-B (Figure 9). Analogs that occupy space shown in the blue region in Figure 8, like the *o*-biphenyl analogs **133** and **138**, display enhanced MAO-A activity and selectivity while analogs that occupy space shown in the green region are inactive. Similarly, analogs that occupy space in the pink region shown in Figure 9, like the *m*-biphenyl analogs **132** and **137**, exhibit enhanced MAO-B selectivity while analogs that occupy space shown in the green region are not MAO-B active. The *p*-biphenyl analogs **131** and **136** occupy space that can be accommodated by neither MAO-A nor MAO-B.

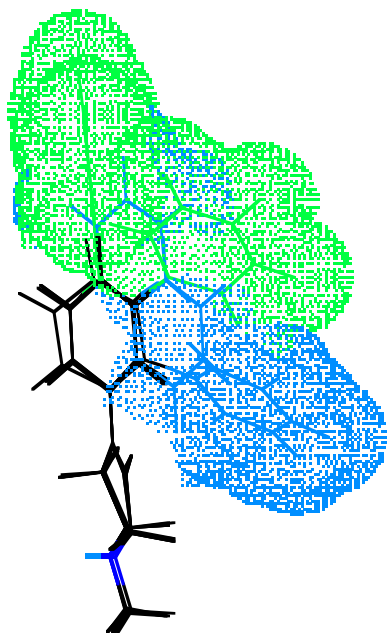


**Figure 8.** MAO-A Active (blue) and Inactive (green) Area.

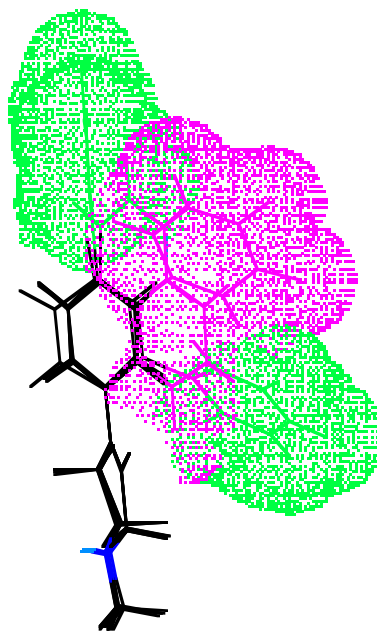


**Figure 9.** MAO-B Active (pink) and Inactive (green) Area.

### 3.5.2. Discussion

As the compounds synthesized in this study are semi-rigid MPTP type analogs (limited flexibility between the carbon C4 and the aryl substituent), the *ortho* and *meta*-biphenyl derivatives can be utilized to obtain new approximations of the size of the active sites. The sizes were measured from the aromatic carbon linked to the C4 position (common atom to all C4 substituents) to the farthest hydrogen of the second phenyl ring (Figure 10). The *o*-biphenyl defines a length of 6.2 Å while the *m*-biphenyl measures 7.5 Å.

These results extend substantially the dimensions of the active sites proposed earlier by Eface.<sup>151</sup> Approximate sizes along the same axes in his models were 5.0 Å in the direction of the *meta* substituent for MAO-B and 4.0 Å in the direction of the *ortho* substituent for MAO-A.

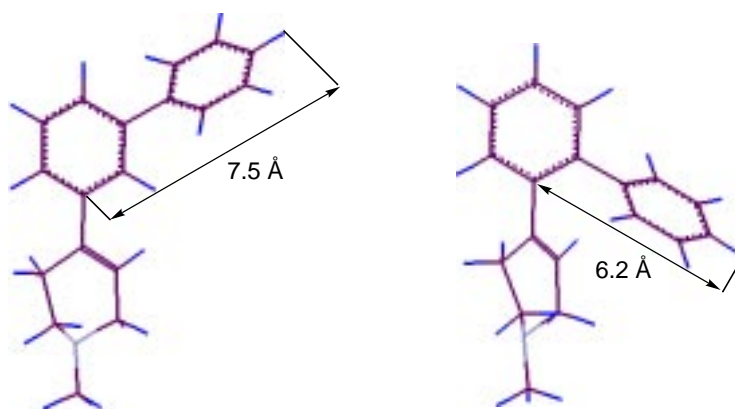


**Figure 10.** Minimum Sizes of MAO-B and MAO-A Active Sites Defined Using Biphenyl Derivatives.

A previous study using a series of substituted 1-methyl-4-phenoxy-1,2,3,6-tetrahydropyridines revealed that the *meta* substituted analogs exhibited MAO-A selectivity. In particular, 1-methyl-4-(3-phenyl)phenoxy-1,2,3,6-tetrahydropyridine (**96**, Chart 3) shows excellent MAO-A activity ( $V_{\max}/K_m = 5568 \text{ min}^{-1}\text{mM}^{-1}$ ) and the highest MAO-A selectivity of the series ( $SC_{A/B} = 8.7$ ). Molecular models with compound **96** and the *o*-biphenyl analog **133** shows that their minimum energy conformers assume very similar geometries (Figure 11).<sup>249</sup> This analysis provides some rationale for the behavior of the two derivatives.

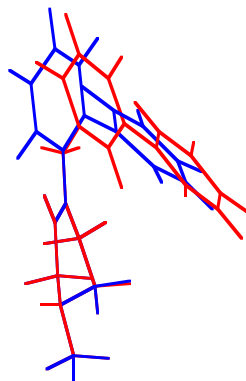


**Figure 11.** Superimposition of the 4-(3-Phenyl)phenoxy (Red) and 4-(2-Phenyl)phenyl (Blue) Derivatives **96** and **133**.

The preliminary topological analysis of these semirigid MPTP analogs discussed here provides some new information about the size limits in the MAO-A and B active sites and is the basis by which we can build updated models of the active sites which incorporate a variety of known 1-methyl-4-substituted-1,2,3,6-tetrahydropyridine substrates. With the preliminary mapping of the active sites we are now able to begin to explain some of the relative enzyme selectivities observed.

### 3.5.3. Validation of topological analysis using tetrahydropyridines

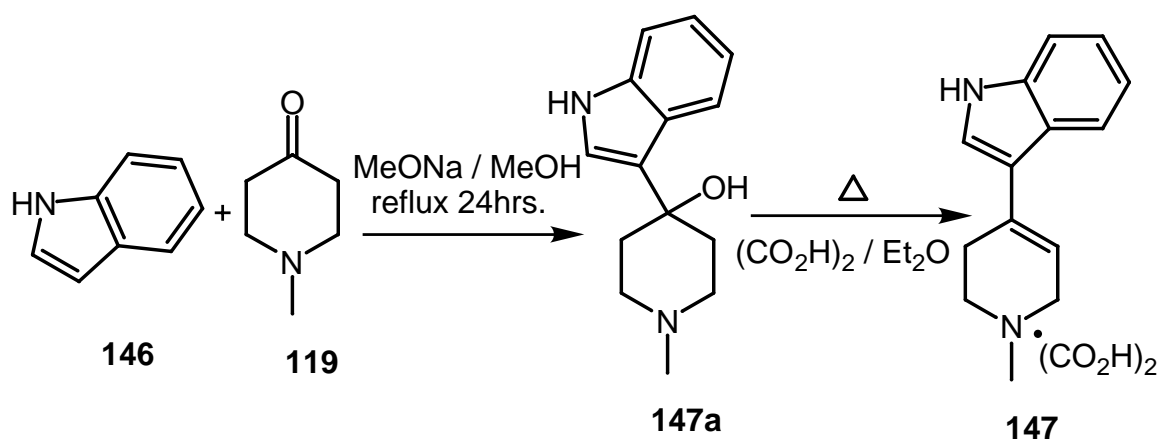
In an attempt to validate the above geometric topological analysis of the MAO-A and MAO-B active sites, the 1-methyl-4-(3-indolyl)-1,2,3,6-tetrahydropyridine derivative (**147**) was investigated. Analog **147** is

geometrically similar to the pure MAO-B substrate 1-methyl-4-(3-methoxyphenyl)-1,2,3,6-tetrahydropyridine (**43**, Table 7). The geometric similarities between these analogs and the preliminary modeling suggest that this analog should be a selective MAO-B substrate experimentally.

### 3.5.4. Synthesis of 1-methyl-4-(3-indolyl)-1,2,3,6-tetrahydropyridine

1-Methyl-4-(3-indolyl)-1,2,3,6-tetrahydropyridine (**147**) was synthesized as reported previously (Scheme 12).<sup>250</sup> Under an anhydrous nitrogen atmosphere, the anion of indole was generated at room temperature using sodium methoxide. The indole anion undergoes condensation with 1-methyl-4-piperidone (**119**) generating a piperidinol intermediate **147a** which undergoes base catalyzed dehydration to yield the tetrahydropyridine **147** directly.

**Scheme 12.** Synthesis of 1-Methyl-4-(3-indolyl)-1,2,3,6-tetrahydropyridine



### 3.5.5. Enzymology

UV scans of a 0.5 mM solution of 1-methyl-4-(3-indolyl)-1,2,3,6-tetrahydropyridine (**147**) in the presence of 0.08  $\mu$ M MAO-B at 30 °C revealed the time-dependent formation of a chromophore with maximal absorption at 425 nm. The kinetic analysis of substrate activity of **147** with 0.08  $\mu$ M MAO-B performed by monitoring the dihydropyridinium product (**148**, Scheme 13) at  $\lambda_{\text{max}} = 425$  nm and monitoring at substrate concentrations of 1.5 mM, 1.0 mM, 0.5 mM, and 0.25 mM (Table 8) established that analog **147** was a good MAO-B substrate. The kinetic parameters were estimated using the  $\epsilon$  value of MPTP (16,000). The Lineweaver-Burke analysis of the data yielded the double reciprocal plot shown in Figure 12, from which we obtained a  $V_{\text{max}}$  and  $K_{\text{m}}$  of 358  $\text{min}^{-1}$  and 0.9 mM, respectively. Taking  $V_{\text{max}}/K_{\text{m}}$  as an overall estimate of the efficiency of catalysis, the substrate activity of **147** was 397  $(\text{min} \cdot \text{mM})^{-1}$ . The scans of **147** with 0.16  $\mu$ M MAO-A at concentrations as high as 3 mM revealed that this analog had no detectable MAO-A substrate properties.

**Table 8a.** The Initial Rates of MAO-B catalyzed conversion of **147** to **148**.

Experiment	1/ [substrate] mM <sup>-1</sup>	Avg. rate (n=2) absorbance/min	Rate nmol/mL · min
A	0.667	0.3718	2065.6
B	1.000	0.2962	1645.6
C	2.000	0.2080	1155.6
D	4.000	0.1259	699.4

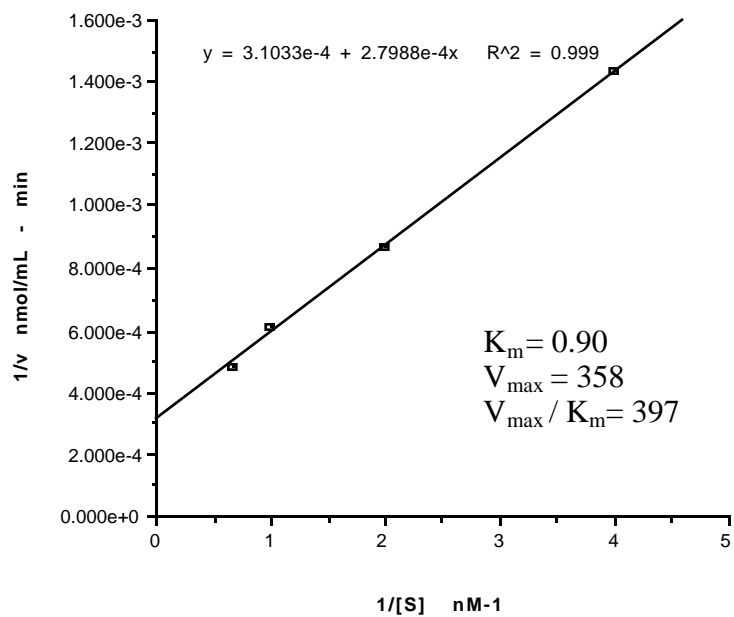
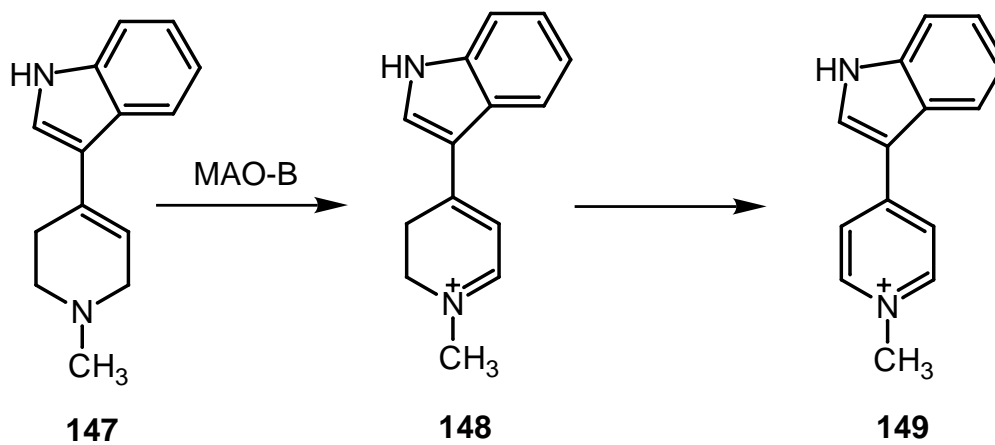


**Figure 12.** The Lineweaver-Burke Double Reciprocal Plot for the MAO-B Catalyzed Oxidation of **147**.

**Scheme 13.** Metabolic Fate of **147** when incubated with MAO-B.



### 3.5.6 Molecular modeling

The 1-methyl-4-(3-indolyl)-1,2,3,6-tetrahydropyridine derivative **147**, a related analog of the neurotoxin MPTP (**3**), proved to be a good MAO-B substrate, as anticipated by its geometry and spatial features (Figure 13B). Based on molecular modeling analysis, this compound was not expected to show MAO-A activity because it points into the region of inactivity defined for MAO-A (Figure 13A - green). Also, a comparison of the dimensions of the indole derivative **147** (5.3 Å) with those of the known MAO-A inactive 3-methoxyphenyl analog **43** (5.4 Å), along the same axis defined above (Figure 14), led to the same prediction. The predictions were confirmed experimentally. Thus, although the indole has quite different electronic and polar characteristics from the aryl hydrocarbon derivatives, its MAO-B/MAO-A selectivity can be predicted based on the topology parameters defined with the hydrocarbon series. As we stated previously,<sup>197</sup> this argues that the molecular geometry is an important determinant in defining the activity and selectivity parameters for MAO-A and MAO-B.

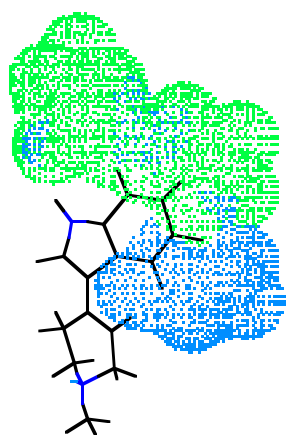


Figure 13A (MAO-A)

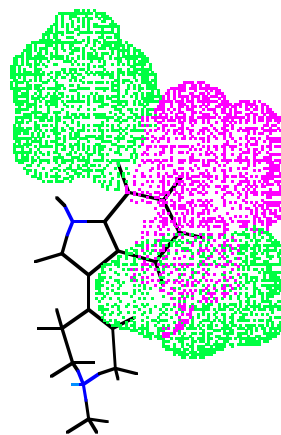
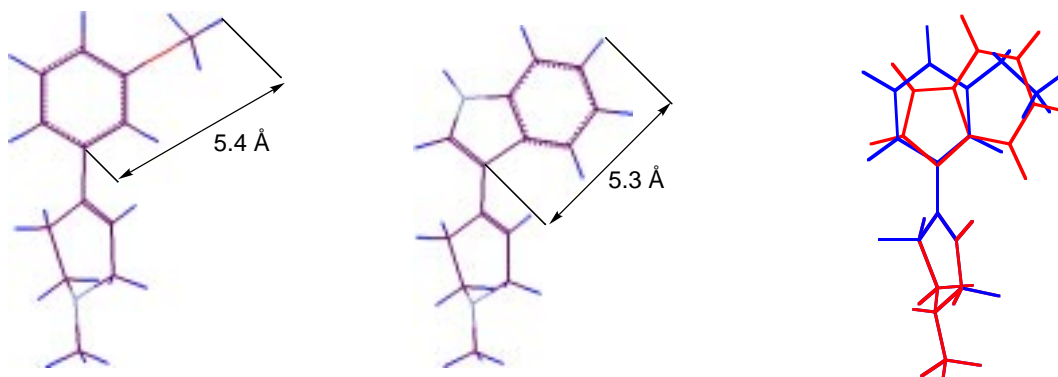


Figure 13B (MAO-B)

**Figure 13 A and B.** Docking of the 3-Indolyl Derivative **147** in MAO-A and MAO-B Active Sites Showing the Interaction with the Inactive Area (green) of MAO-A.



**Figure 14.** Comparison of the Sizes of 3-Methoxyphenyl **43** (blue) and 3-Indolyl **147** (red) Derivatives.

Using a rather simple topological analysis based on the results obtained with a series of hydrocarbon aryl analogs, the selectivity of various types of C4-substituted tetrahydropyridines derivatives can be rationalized and predicted. Our results provide additional information that can be used to refine the molecular modeling results reported by Efange *et al.*<sup>151</sup> and the comparative molecular field analyses (CoMFA) developed by Testa and Carrupt<sup>195,196</sup> on 1,4-disubstituted tetrahydropyridine derivatives.